Lattice symmetries and regular magnetic orders in classical frustrated antiferromagnets

L. Messio, C. Lhuillier, and G. Misguich

Phys. Rev. B **83**, 184401 — Published 6 May 2011

DOI: 10.1103/PhysRevB.83.184401

Lattice symmetries and regular magnetic orders in classical frustrated antiferromagnets

L. Messio,[1] C. Lhuillier,[2] and G. Misguich,[3]
1.*Institute of Theoretical Physics, Ecole Polytechnique Fédérale de Lausanne, CH-1015 Lausanne, Switzerland.*
2.*Laboratoire de Physique Théorique de la Matière Condensée, UMR 7600 CNRS, Université Pierre et Marie Curie, Paris VI, 75252 Paris Cedex 05, France.*
3.*Institut de Physique Théorique, CNRS, URA 2306, CEA, IPhT, 91191 Gif-sur-Yvette, France.*
(Dated: March 8, 2011)

We consider some classical and frustrated lattice spin models with global $O(3)$ spin symmetry. No general analytical method to find a ground-state exists when the spin dependence of the Hamiltonian is more than quadratic (i.e. beyond the Heisenberg model) and/or when the lattice has more than one site per unit cell. To deal with these cases, we introduce a family of variational spin configurations, dubbed "regular magnetic orders" (RMOs), which respect all the lattice symmetries *modulo global* $O(3)$ *spin transformations* (rotations and/or spin flips). The construction of these states is explicited through a group theoretical approach and all the RMOs on the square, triangular, honeycomb and kagome lattices are listed. Their equal time structure factors and powder-averages are shown for comparison with experiments. Well known Néel states with 1, 2 or 3 sublattices on various lattices are RMOs, but the RMOs also encompass exotic non-planar states with cubic, tetrahedral or cuboctahedral geometry of the $T = 0$ order parameter. Whatever the details of the Hamiltonian (with the same symmetry group), a large fraction of these RMOs are energetically stationary with respect to small deviations of the spins. In fact these RMOs appear as exact ground-states in large domains of parameter space of simple models that we have considered. As examples, we display the variational phase diagrams of the J_1-J_2-J_3 Heisenberg model on all the previous lattices as well as that of the J_1-J_2-K ring-exchange model on square and triangular lattices.

PACS numbers: 75.10.Hk,75.40.Cx

I. INTRODUCTION

Finding the ground-state (GS) of an antiferromagnetic *quantum* spin model is a notoriously difficult problem. Moreover, even *classical* spin models at zero temperature can be non-trivial to solve, unless one carries some extensive numerical investigation. In particular there is no general method to determine the lowest energy configurations for a simple Heisenberg $O(3)$ model of the type

$$E = \sum_{i,j} J(|\mathbf{x}_i - \mathbf{x}_j|)\mathbf{S}_i \cdot \mathbf{S}_j \qquad (1)$$

if the lattice sites $\{\mathbf{x}_i\}$ do *not* form a Bravais lattice. It is only if there is a single site per unit cell (Bravais lattice) that one can easily construct some GS[1] (see Sec. VI B).

Another situation where the classical energy minimization is not simple is that of multiple-spin interactions, where the energy is not quadratic in the spin components. Finding the GS in presence of interactions of the type $(\mathbf{S}_i \cdot \mathbf{S}_j)(\mathbf{S}_k \cdot \mathbf{S}_l)$ can be difficult and, in general, has to be done numerically even on Bravais lattices. Such terms arise in the classical limit of ring-exchange interactions. For instance, the – apparently simple – classical model with Heisenberg interactions competing with four-spin ring-exchange on the triangular lattice is not completely solved.[2]

In this study, we introduce and construct a family of spin configurations, dubbed "regular magnetic orders" (RMO). These configurations are those which respect all the symmetries of a given lattice *modulo global spin transformations* (rotations and/or spin flips). This property is obeyed by most usual Néel states. For instance, the two- (resp. three-) sublattice Néel state on the square (resp. triangular) lattice, GS of the antiferromagnetic first neighbor Hamiltonian, respects the lattice symmetries: each symmetry operation can be "compensated" by the appropriate global spin rotation of angle 0 or π (resp. 0, $\pm 2\pi/3$).

By definition, the set of RMOs only depends on the symmetries of the model – the lattice symmetries and the spin symmetries – and therefore does not depend on the strength of the different interactions ($J(|\mathbf{x}|)$ in the example of Eq. (1)). These states comprise well-known structures, like the two and three sublattice Néel states mentioned above, but also some new states, like non-planar structures on the kagome lattice that will be discussed in Sec. IV A.

The reason why these states are interesting for the study of frustrated antiferromagnets is that they are good "variational candidates" to be the ground-state of many specific models. In fact, rather surprisingly, we found that these states (together with spiral states) exhaust all the GS in a large range of parameters of the frustrated spin models we have investigated. For instance, in the case of an Heisenberg model on the kagome lattice (studied in Sec. VI C) with competing interactions between first, second and third neighbors, some non-planar spin structures (based on cuboctahedron) turn out to be stable phases. In other words, the set of RMOs and spiral states form a good starting point to determine the phase diagram of a classical $O(3)$ model, without having

to resort to lengthy numerical minimizations.[33] In several cases, we even observed that one of the RMOs reaches an exact energy lower bound, therefore proving that it is one (maybe not unique) GS of the model.

These states may also be used when analyzing experimental data on magnetic compounds where the lattice structure is known, but where the values (and range) of the magnetic interactions are not. In such a case, the (equal time) magnetic correlations – measured by neutron scattering – can directly be compared to those of the RMOs. If these correlations match those of one RMO, this may be used, in turn, to get some information about the couplings. With this application in mind, we provide the magnetic structure factors of all the RMOs we construct and powder-averages of some of them (see App. B).

The organization of the paper is as follows: in Sec. II we present the definition of a RMO, a state that weakly breaks the lattice symmetries and all the notations needed for the group theoretical approach. In Sec. III A, we explain the algebraic structure of the group of joint space- and spin-transformations that leave a regular spin configuration invariant (algebraic symmetry group) and describe it for the triangular lattice (detailed calculations are given in App. A). We then explain how to construct RMOs in Sec. III B. This approach is algebraically very similar to Wen's construction of symmetric spin liquids,[3] but there are also strong differences in the invariance requirements: whereas the symmetric spin liquids do not break lattice symmetries (they are "liquids"), our RMOs indeed break lattice symmetries but in a "weak" way (see App. C). These sub-sections are self-contained, but can be skipped by readers interested essentially in the results. In Sec. III C, we construct all the RMOs on the triangular lattice. In sections Sec. IV A and IV B we list the RMOs on the kagome and honeycomb lattices (which have the same algebraic symmetry group as the triangular lattice), and with a minimum of algebra we present the RMOs on the square lattice (Sec. IV C). We then show that spiral states can be seen in this picture as RMOs with a lattice symmetry group reduced to the translation group (Sec. IV D). In Sec. V we discuss geometrical properties of RMOs and the relationship between RMOs and representations of the lattice symmetry group. This section can be skipped by readers more interested in physics than in geometry. In Sec. VI we study the energetics of these RMOs and therefore their interest for the variational description of the $T = 0$ phase diagrams of frustrated spin models. We first show in Sec. VI A that all RMOs which do not belong to a continuous family are energetically stationary with respect to small spin deviations and thus good GS candidates for a large family of Hamiltonians. After having given a lower bound on the energy of Heisenberg models (Sec. VI B), we then show that over a large range of coupling constants the RMOs are indeed exact GSs of the J_1-J_2-J_3 model on the honeycomb and kagome lattices (Sec. VI C). We then display in Sec. VI D a variational phase diagram of the J_1-J_2-K model on square and triangular lattices. In Sec. VI E we discuss finite temperature phase transitions: the non planar states are chiral and should give rise to a $T \neq 0$ phase transition. Sec. VII is our conclusion.

The calculation of the algebraic symmetry groups on the triangular lattice is detailed in App. A. Powder-averages of the structure factors of the RMOs on triangular and kagome lattices are displayed in App. B. Analogies and differences between the present analysis and Wen's analysis of quantum spin models are explained in App. C.

II. NOTATIONS AND DEFINITIONS

We will mostly concentrate on Heisenberg-spin models where on each lattice site i, the spin $\mathbf{S}_i$ is a three component unit vector. But the concept of RMO can be easily extended to the general situation where $\mathbf{S}_i$ belongs to an other manifold $\mathcal{A}$ (as for example for nematic or quadrupolar order parameters as encountered in some quantum systems).

We note by S_S the group of the "global spin symmetries" of the Hamiltonian. In the general framework, an element of S_S is a mapping of $\mathcal{A}$ onto itself which does not change the energy of the spin configurations. For an Heisenberg model without applied magnetic field, S_S is simply (isomorphic to) the orthogonal group $O(3)$. In a similar way, we note by S_L the lattice symmetry group of the Hamiltonian. An element of S_L acts on spin configurations by mapping the lattice L onto itself and is the identity in the spin space $\mathcal{A}$.

In this paper, we will restrict ourselves to the (rather common) situation where the full symmetry group S_H of the model is the direct product $S_S \times S_L$.[34]

Let $\mathcal{G}$ be the set of all the applications from the lattice symmetry group S_L to the spin symmetry group S_S. An element G of $\mathcal{G}$ associates a spin symmetry G_X to each lattice symmetry X:

$$\begin{aligned} G : S_L &\to S_S \\ X &\mapsto G_X \end{aligned} \tag{2}$$

We now concentrate on a fixed spin configuration c. We note H_c its stabilizer, that is the subgroup of S_H which elements do not modify c. Its spin symmetry group H_c^S is the group of unbroken spin symmetries: $H_c^S = S_S \cap H_c$.

Definitions:

- *A mapping $G \in \mathcal{G}$ is said to be compatible with a spin configuration c if the composition of an element of S_L with its image by G leaves c unchanged:*

$$\forall X \in S_L, \quad G_X X \in H_c. \tag{3}$$

- *A configuration c is said to be regular if any lattice symmetry $X \in S_L$ can be "compensated" by an appropriate spin symmetry $G_X \in S_S$, which means $G_X X|c\rangle = |c\rangle$ (that is $G_X X \in H_c$).* In other words, *c is a RMO if there exists a mapping $G \in \mathcal{G}$ such that G and c are compatible.*

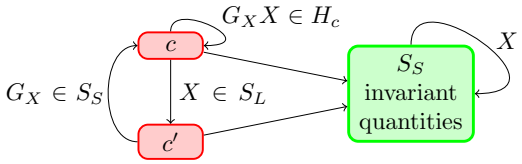

FIG. 1: (Color online) A lattice symmetry $X \in S_L$ acts on a spin configuration c to give a new configuration $c' = Xc$. If c is regular, there is a spin symmetry $G_X \in S_S$ such that one gets back the initial state: $G_X c' = c$.

In a RMO, the observables which are invariant under S_S are therefore invariant under all lattice symmetries. These definitions are summarized in Fig. 1.

The simplest RMOs are those which are already invariant under lattice symmetries (i.e. $S_L \subset H_c$), without the need to perform any spin symmetry. This is the case of a ferromagnetic (F) configuration, with all spins oriented in the same way. But less trivial possibilities exist, as the classical GS of the antiferromagnetic (AF) first neighbor Heisenberg interaction on the square lattice. This GS possesses two sublattices with opposite spin orientations. Each lattice symmetry X either conserves the spin orientations, or reverses them, so we can choose as G_X either the identity or the spin inversion $\mathbf{S}_i \to -\mathbf{S}_i$.

If the subgroup $H_c^S = S_S \cap H_c$ of unbroken spin symmetries contains more than the identity, there are several elements of $\mathcal{G}$ compatible with c. For each X, they are as many G_X as elements in H_c^S. In the previous example of the GS of the AF square lattice, H_c^S is the set of spin transformations that preserve the two opposite spins orientations: this group is isomorph to $O(2)$. Beginning with a compatible G, each G_X can be composed with an element of H_c^S to give an other compatible element of $\mathcal{G}$.

To summarize, RMOs are not restricted to states strictly respecting the lattice symmetries, but to states that in some way *weakly* respect them. We will now explain how to construct *all* the regular spin configurations on a given lattice.

III. CONSTRUCTION OF RMOS

To construct the RMOs, we proceed in two steps. *In the first step, we fix a given unbroken spin symmetry group* H_c^S, and consider the algebraic constraints that the lattice symmetry group S_L imposes on a mapping $G \in \mathcal{G}$, assuming that some (so far unknown) spin configuration c is compatible with G. These constraints lead to a selection of a subset $\mathcal{G}^A$ of $\mathcal{G}$, composed of the mappings G which are compatible with the lattice symmetries. For an element G of $\mathcal{G}^A$, the group

$$H^G = \{G_X X, X \in S_L\} \times H_c^S, \tag{4}$$

is dubbed the *algebraic symmetry group* associated to G.

When $H_c^S = \{I\}$, the algebraic symmetry groups are an extension of the magnetic space groups[18] which are themselves an extension of the crystallographic space groups. To go from crystallographic to magnetic space groups, the time reversal transformation or the identity is combined to each of the lattice transformations. Points of the lattice wear black or white points. To go from crystallographic to algebraic symmetry groups, it is a spin transformation which is combined to each of the lattice transformations. Now points of the lattice wear elements of S_S.

In 3D, there are 230 crystallographic space groups. In 2D, they reduce to the 17 wallpaper groups. In the following sections, we are going to derive all the algebraic symmetry groups derived from two of the wallpaper groups, denoted $p6m$ (triangular Bravais lattice of Fig. 2) and $p4m$ (square Bravais lattice of Fig. 2) in the Hermann-Mauguin notations. These are the simplest cases in 2D because the most constrained, thus with the least number of groups. But we could derive the algebraic symmetry group of any of the 2D or 3D crystallographic space groups by the same procedure as in these examples.

In the second step of the RMO construction, one determines the configurations (if any) which are compatible with a given algebraic symmetry group.

A. Algebraic symmetry groups

We fix the spin symmetry group H_c^S (to be exhaustive, we will consecutively consider each possible H_c^S). Let X, Y and Z, three elements of S_L such that $XY = Z$. We will see that this algebraic relation imposes some constraints on the mappings G which are compatible with a spin configuration. Indeed, we assume that there exists a configuration c compatible with G. Then, $G_Z Z$ and $G_X X G_Y Y$ are in H_c. This implies that $G_X X G_Y Y Z^{-1} G_Z^{-1}$ is also in H_c. Elements of S_L and S_S commute, so we have $G_X X G_Y Y Z^{-1} G_Z^{-1} = G_X G_Y G_Z^{-1}$, which is a pure spin transformation. We deduce that

$$\forall X, Y \in S_L, \quad G_X G_Y G_{(XY)}^{-1} \in H_c^S. \tag{5}$$

If the constraint above is not satisfied, G must be excluded from the set $\mathcal{G}^A$ of the algebraically compatible mappings.

Now we illustrate these general considerations using the following example: L is an infinite triangular lattice and the spin space $\mathcal{A}$ is the two-dimensional sphere $\mathcal{S}_2$ (Heisenberg spins). S_L is generated by two translations T_1 and T_2 along vectors $\mathbf{T}_1$ and $\mathbf{T}_2$, a reflexion σ and a rotation R_6 of angle $\pi/3$, described in Fig. 2 and defined in the $(\mathbf{T}_1, \mathbf{T}_2)$ basis as:

$$T_1 : (r_1, r_2) \mapsto (r_1 + 1, r_2) \tag{6a}$$
$$T_2 : (r_1, r_2) \mapsto (r_1, r_2 + 1) \tag{6b}$$
$$\sigma : (r_1, r_2) \mapsto (r_2, r_1) \tag{6c}$$
$$R_6 : (r_1, r_2) \mapsto (r_1 - r_2, r_1). \tag{6d}$$

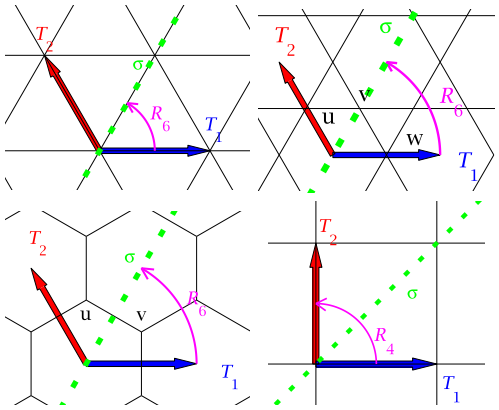

FIG. 2: (Colour online) Generators of the lattice symmetries group S_L for the triangular, kagome, honeycomb and square lattices. For the first three lattices : the two translations T_1 and T_2 (along the two basis vectors $\mathbf{T}_1$ and $\mathbf{T}_2$), the reflexion σ an the rotation R_6 of angle $\pi/3$. For the square lattice, generators of S_L are T_1, T_2, σ an the rotation R_4 of angle $\pi/2$.

The spin symmetry group S_S is chosen to be $O(3)$ (as for an Heisenberg model). In such a system, the unbroken symmetry group H_c^S is either isomorph to $\{I\}$, $\mathbb{Z}_2$ or $O(2)$, depending on the orientations of the spins (non-coplanar, coplanar or colinear respectively). The non-planar case, $H_c^S = \{I\}$, is the most interesting case and we choose it for this example. The two other cases can be treated by reducing $\mathcal{A}$ to the circle $\mathcal{S}_1$ or $\mathcal{S}_0 = \{1, -1\}$ (XY or Ising spins) and S_S to $O(2)$ or $O(1)$ in order to have $H_c^S = \{I\}$, which considerably simplifies the calculations.

We assume that a mapping G belongs to $\mathcal{G}^A$ (algebraically compatible). As $H_c^S = \{I\}$, Eq. (5) allows to construct the full mapping G simply from the images of the generators of the lattice symmetry group S_L. As several combinations of generators can produce the same element of S_L, the images by G of the S_L generators must satisfy some algebraic relations. These relations where needed in a similar algebraic study in Ref. 4 and consist in all the relations necessary to put each product of generators in the form $\sigma^s R_6^r T_1^{t_1} T_2^{t_2}$, where $s = 0, 1$, $r = 0, 1, ..., 5$ and t_1, $t_2 \in \mathbb{Z}$. These relations are:

$$T_1 T_2 = T_2 T_1 \tag{7a}$$
$$T_1 R_6 T_2 = R_6 \tag{7b}$$
$$R_6 T_1 T_2 = T_2 R_6 \tag{7c}$$
$$T_1 \sigma = \sigma T_2 \tag{7d}$$
$$R_6^6 = I \tag{7e}$$
$$\sigma^2 = I \tag{7f}$$
$$R_6 \sigma R_6 = \sigma. \tag{7g}$$

From these equations and from Eq. (5) we get:

$$G_{T_1} G_{T_2} = G_{T_2} G_{T_1} \tag{8a}$$
$$G_{T_1} G_{R_6} G_{T_2} = G_{R_6} \tag{8b}$$
$$G_{R_6} G_{T_1} G_{T_2} = G_{T_2} G_{R_6} \tag{8c}$$
$$G_{T_1} G_\sigma = G_\sigma G_{T_2} \tag{8d}$$
$$G_{R_6}^6 = I \tag{8e}$$
$$G_{\sigma^2} = I \tag{8f}$$
$$G_{R_6} G_\sigma G_{R_6} = G_\sigma. \tag{8g}$$

The details of the calculations are given in App. A. The solutions can be divided in three families:

$$G_{T_1} = G_{T_2} = I, \tag{9a}$$
$$\theta_{T_1} = \theta_{T_2} = \pi \text{ and } \mathbf{n}_{T_1} \perp \mathbf{n}_{T_2}, \tag{9b}$$
$$G_{T_1} = G_{T_2} \neq I, \tag{9c}$$

where each element G_X is characterised by its determinant $\varepsilon_X = \pm 1$ (not appearing here) and by a rotation $R_{\mathbf{n}_X \theta_X}$ of axis $\mathbf{n}_X$ and of angle $\theta_X \in [0, \pi]$ such that $G_X = \varepsilon_X R_{\mathbf{n}_X \theta_X}$. Up to a global similarity relation ($G_X \to M G_X M^{-1}$, $M \in SO(3)$), we obtain 28 solutions of the system of Eqs. (8) in the case of Eq. (9a), 4 for Eq. (9b) and 8 for Eq. (9c). The 40 solutions are listed below :

$$G_{T_1} = G_{T_2} = I, G_\sigma = \varepsilon_\sigma I, G_{R_6} = \varepsilon_R I, \tag{10a}$$
$$G_{T_1} = G_{T_2} = I, G_\sigma = \varepsilon_\sigma I, G_{R_6} = \varepsilon_R R_{\mathbf{z}\pi}, \tag{10b}$$
$$G_{T_1} = G_{T_2} = I, G_\sigma = \varepsilon_\sigma R_{\mathbf{z}\pi}, G_{R_6} = \varepsilon_R I, \tag{10c}$$
$$G_{T_1} = G_{T_2} = I, G_\sigma = \varepsilon_\sigma R_{\mathbf{z}\pi}, G_{R_6} = \varepsilon_R R_{\mathbf{z}\pi}, \tag{10d}$$
$$G_{T_1} = G_{T_2} = I, G_\sigma = \varepsilon_\sigma R_{\mathbf{z}\pi}, G_{R_6} = \varepsilon_R R_{\mathbf{x}\pi}, \tag{10e}$$
$$G_{T_1} = G_{T_2} = I, G_\sigma = \varepsilon_\sigma R_{\mathbf{z}\pi}, G_{R_6} = \varepsilon_R R_{\mathbf{x}\theta}, \tag{10f}$$
$$G_{T_1} = R_{\mathbf{x}\pi}, G_{T_2} = R_{\mathbf{y}\pi}, \quad G_\sigma = -\varepsilon_\sigma \begin{pmatrix} 0&1&0 \\ 1&0&0 \\ 0&0&1 \end{pmatrix}, G_{R_6} = \varepsilon_R \begin{pmatrix} 0&1&0 \\ 0&0&1 \\ 1&0&0 \end{pmatrix}, \tag{10g}$$
$$G_{T_1} = G_{T_2} = R_{\mathbf{z}\frac{2\pi}{3}}, G_\sigma = \varepsilon_\sigma I, G_{R_6} = \varepsilon_R R_{\mathbf{x}\pi}, \tag{10h}$$
$$G_{T_1} = G_{T_2} = R_{\mathbf{z}\frac{2\pi}{3}}, G_\sigma = \varepsilon_\sigma R_{\mathbf{z}\pi}, G_{R_6} = \varepsilon_R R_{\mathbf{x}\pi}. \tag{10i}$$

where $\mathbf{x} \perp \mathbf{z}$, ε_σ, $\varepsilon_R = \pm 1$ and $\theta \in \left\{\frac{\pi}{3}, \frac{2\pi}{3}\right\}$. Each line corresponds to 4 solutions, except Eq. (10f) with 8 solutions. We stress that the algebraic symmetry groups depend on S_S, H_c^S and on the algebraic properties of S_L, but not directly on the lattice L. In particular, different lattices can have the same algebraic symmetry groups. The results Eqs. 10 are exactly the same on a honeycomb or a kagome lattice with symmetries of Fig. 2 because the algebraic equations Eqs. 7 stay the same.

B. Compatible states

The second step consists in taking each element of $\mathcal{G}^A$ and finding all the compatible states. This last step is fully lattice dependent.

To construct a RMO compatible with some mapping $G \in \mathcal{G}^A$, one first chooses the direction of the spin on a site i. Then, by applying all the transformations of S_L, we deduce the spin directions on the other sites. A constraint appears when two different transformations X and Y lead to the same site $X(i) = Y(i)$. The image spins have to be the same: $G_X(\mathbf{S}_i) = G_Y(\mathbf{S}_i)$. It can either give a constraint on the direction of $\mathbf{S}_i$, either indicate that no $G-$compatible state exists.

To find these constraints, we divide the lattice sites in orbits under the action of S_L (if all the sites are equivalent, there is a single orbit). In each orbit, we choose a site i. Each non trivial transformation X that does not displace i gives a constraint: $G_X(\mathbf{S}_i) = \mathbf{S}_i$. For each $G \in \mathcal{G}^A$, the associated RMOs are obtained by choosing a site in each orbit, a spin direction respecting the site constraints and then propagating the spin directions through the lattice using the symmetries in S_L.

C. Example of RMO construction: the triangular lattice

Let us apply this method to the example of the triangular lattice. There is a single orbit, and the transformations that leave invariant the site of coordinates $(0,0)$ in the $(\mathbf{T}_1, \mathbf{T}_2)$ basis (see Fig. 2) are generated by σ and R_6, giving the two constraints $G_\sigma(\mathbf{S}(0,0)) = G_{R_6}(\mathbf{S}(0,0)) = \mathbf{S}(0,0)$.

The mapping of Eq. (10a) has compatible states only for $\varepsilon_R = \varepsilon_\sigma = 1$. They are ferromagnetic (F) states, as shown in Fig. 3(a). Since $G_{T_{1-2}} = I$ for the Eqs. (10b)-(10f), no new RMOs can be compatible with any of them.

The mapping of Eq. (10g) has compatible states only for $\varepsilon_R = 1$ and $\varepsilon_\sigma = -1$. Then $\mathbf{S}(0,0) = \pm(1,1,1)/\sqrt{3}$ and the state is the tetrahedral state depicted in Fig. 3(b), where the spins of four sublattices point toward the corners of a tetrahedron. The sign of $\mathbf{S}(0,0)$ determines the chirality of the configuration.

The next RMO is the coplanar state of Fig. 3(c), which is compatible with Eq. (10i) for $\varepsilon_R = \varepsilon_\sigma = 1$ and $\mathbf{S}(0,0) = \pm(1,0,0)$. The three sublattices are coplanar with relative angles of 120°. This state is not chiral because the configurations obtained with the two possible $\mathbf{S}(0,0)$ are related by a global spin rotation in $SO(3)$.

A continuum of *umbrella* states are compatible with Eq. (10i) with $\varepsilon_\sigma = 1$ and $\varepsilon_R = -1$. They are depicted in Fig. 3(d), where the sublattices are the same than for the coplanar states but the relative angles between the spin orientations are all identical and $\leq 120°$. This family interpolates between the F and the coplanar states.

We started by choosing $H_c^S = \{I\}$, but states with $H_c^S = \mathbf{Z}_2$ (for the coplanar state) or $O(2)$ (for the F state) have been obtained anyway. One can check that choosing another H_c^S would not give any new RMO. All the RMOs are thus those gathered in Fig. 3.

The Bragg peaks of these states are displayed in the hexagonal Brillouin zone in the right column of Fig. 3

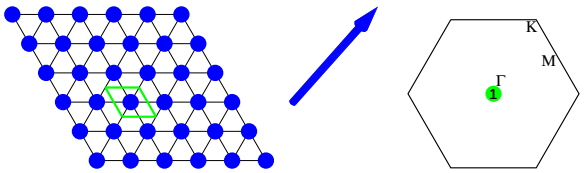

(a) Ferromagnetic (F) state. $E = 6J_1 + 6J_2 + 6J_3 + 42K$.

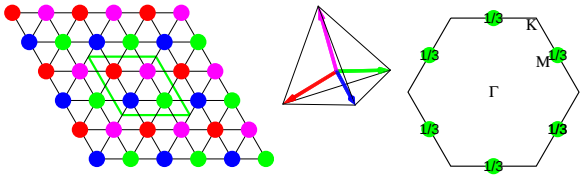

(b) Tetrahedral state. $E = -2J_1 - 2J_2 + 6J_3 - 34K/3$.

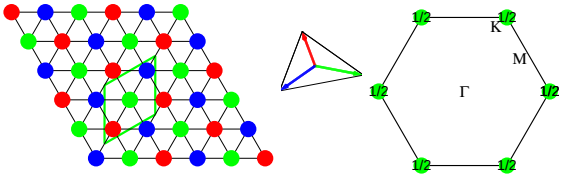

(c) Coplanar state. $E = -3J_1 + 6J_2 - 3J_3 - 3K$.

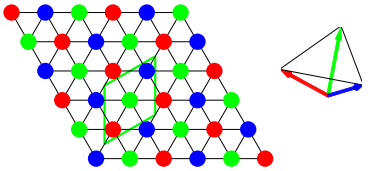

(d) F umbrella states.

FIG. 3: (Color online) Regular magnetic orders on the triangular lattice. The sublattice arrangements (labelled by colors) and the spin directions on each sublattice are displayed in the left and center columns. A spin unit cell is surrounded with green lines. The positions and weights of the Bragg peaks in the hexagonal Brillouin zone of the lattice are in the right column. The energy per site of each structure is given as a function of the parameters of the models described in Sec VI.

and their powder-averaged structure factors in App. B together with the formulas for these quantities.

IV. REGULAR MAGNETIC ORDERS FOR HEISENBERG SPINS ON SEVERAL SIMPLE LATTICES

In the following we enumerate the RMOs on the kagome and honeycomb lattices, two lattices which have a symmetry group S_L isomorphic to that of the triangular lattice. To be complete, we also present the RMOs on the square lattice and discuss the spiral states that may be seen as RMOs when S_L reduces to the translation group.

A. Kagome lattice

The symmetry group S_L of the kagome lattice is isomorphic to that of the triangular lattice, thus the algebraic solutions Eqs. (10) remain valid. Carrying out the approach of Sec. III B for this new lattice, one obtains all the RMOs on the kagome lattice. They are displayed in Fig. 4 together with the positions and weights of the Bragg peaks and are listed below. The equal time structure factor is depicted in the Extended Brillouin Zone (EBZ), drawn with thin lines in Fig. 4: the kagome lattice has 3 sites per unit cell of the underlying triangular lattice and the EBZ has a surface four times larger than the BZ of the underlying triangular Bravais lattice, drawn with dark lines. Powder-averaged structure factors of the RMOs are given in App. B.

One RMO is colinear ($H_c^S = O(2)$):

- the ferromagnetic (F) state of Fig. 4(a).

Two states with a zero total magnetization are coplanar ($H_c^S = \mathbb{Z}_2$):

- the $\mathbf{q} = \mathbf{0}$ state of Fig. 4(b) has 3 sublattices of spins at 120° and a 3 sites unit cell,
- the $\sqrt{3} \times \sqrt{3}$ state of Fig. 4(c) has 3 sublattices of spins at 120° and a 9 sites unit cell.

Three states with a zero total magnetization completely break $O(3)$ ($H_c^S = \{I\}$):

- the octahedral state of Fig. 4(d) has 6 sublattices of spins oriented toward the corners of an octahedra and a 12 sites unit cell,
- the cuboc1 state of Fig. 4(e) has 12 sublattices of spins oriented toward the corners of a cuboctahedron and a 12 sites unit cell,
- the cuboc2 state of Fig. 4(f) has 12 sublattices of spins oriented toward the corners of an cuboctahedron and a 12 sites unit cell. Note that the first neighbor spins have relative angles of 60°, in contrast to 120° for the cuboc1 state.

Two continua of states with a non-zero total magnetization completely break $O(3)$ ($H_c^S = \{I\}$):

- the $\mathbf{q} = \mathbf{0}$ umbrella states of Fig. 4(g), left,
- the $\sqrt{3} \times \sqrt{3}$ umbrella states of Fig. 4(g), right.

These continua interpolate between the ferromagnetic state and the coplanar states Fig. 4(b) and Fig. 4(c).

B. Honeycomb lattice

All the RMOs on the honeycomb lattice are depicted in Fig. 5 and listed below. The EBZ is drawn with thin lines (its surface is three times larger than that of the BZ).

Two RMOs are colinear ($H_c^S = O(2)$):

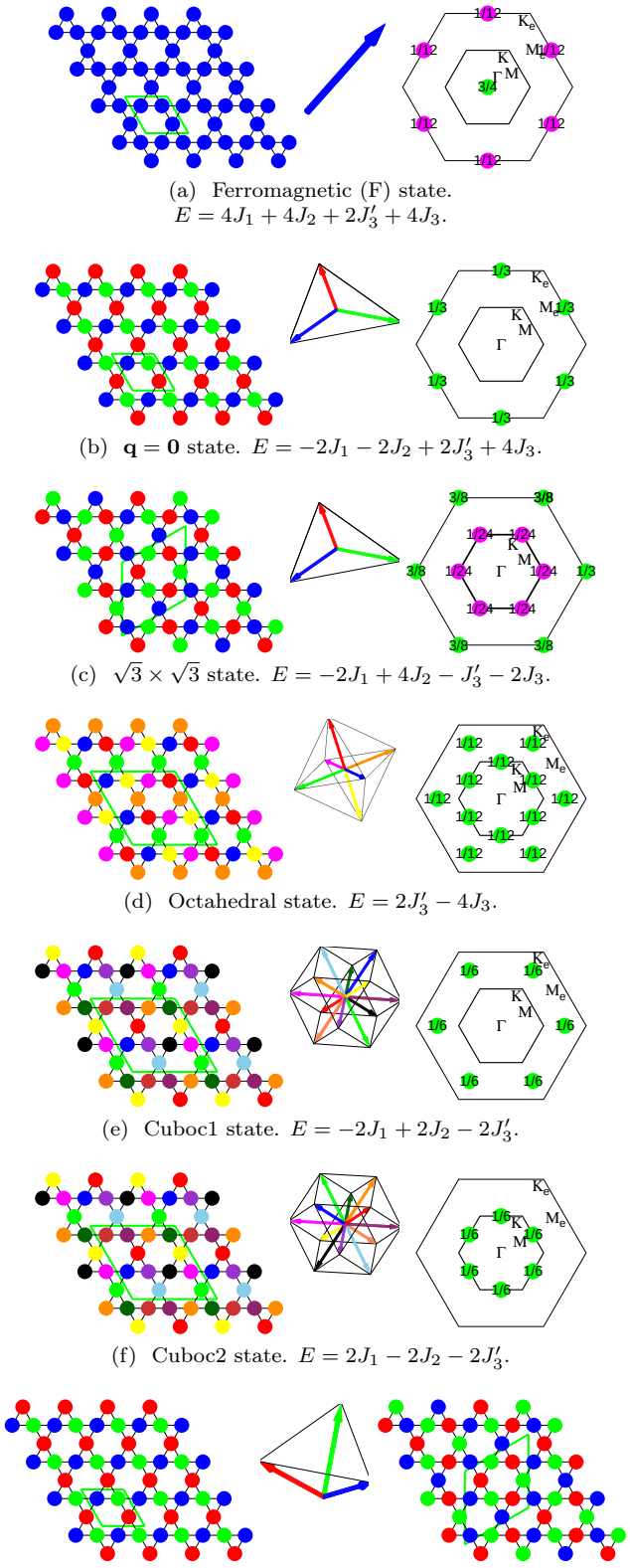

(a) Ferromagnetic (F) state. $E = 4J_1 + 4J_2 + 2J_3' + 4J_3$.

(b) $\mathbf{q} = \mathbf{0}$ state. $E = -2J_1 - 2J_2 + 2J_3' + 4J_3$.

(c) $\sqrt{3} \times \sqrt{3}$ state. $E = -2J_1 + 4J_2 - J_3' - 2J_3$.

(d) Octahedral state. $E = 2J_3' - 4J_3$.

(e) Cuboc1 state. $E = -2J_1 + 2J_2 - 2J_3'$.

(f) Cuboc2 state. $E = 2J_1 - 2J_2 - 2J_3'$.

(g) $\mathbf{q} = \mathbf{0}$ (left) and $\sqrt{3} \times \sqrt{3}$ (right) umbrella states.

FIG. 4: (Color online) Regular magnetic orders on the kagome lattice and their equal time structure factors in the EBZ (see text). The energies (per site) of these states are given for the J_1-J_2-J_3-J_3' model described in Sec VI.

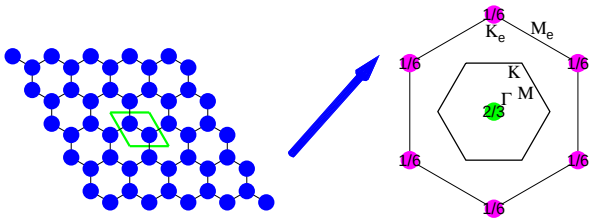

(a) Ferromagnetic (F) state. $E = 3J_1 + 6J_2 + 3J_3$.

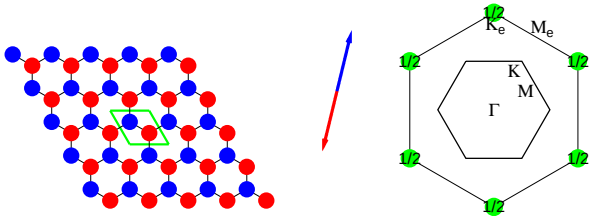

(b) Antiferromagnetic (AF) state. $E = -3J_1 + 6J_2 - 3J_3$.

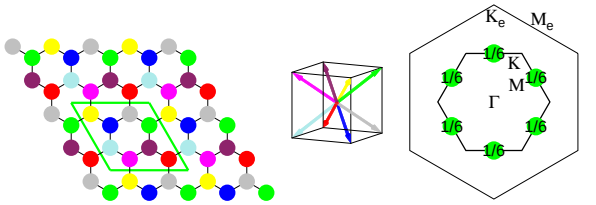

(c) Cubic state. $E = J_1 - 2J_2 - 3J_3$.

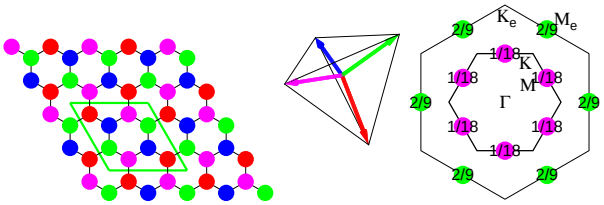

(d) Tetrahedral state. $E = -J_1 - 2J_2 + 3J_3$.

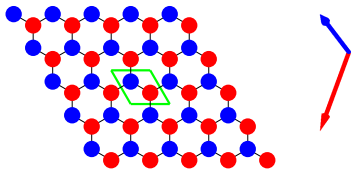

(e) V states.

FIG. 5: (Color online) Regular magnetic orders on the honeycomb lattice and their equal time structure factors in the EBZ (see text). The energies (per site) are given for a J_1-J_2-J_3 Heisenberg model.

- the ferromagnetic state of Fig. 5(a),
- the antiferromagnetic state of Fig. 5(b) has 2 sublattices of spins oriented in opposite directions and a 2 sites unit cell.

Two states with a zero total magnetization completely break $O(3)$ ($H_c^S = \{I\}$):

- the cubic state of Fig. 5(c) has 8 sublattices of spins oriented toward the corners of a cube and a 8 sites unit cell,
- the tetrahedral state of Fig. 5(d) has 4 sublattices of spins oriented toward the corners of a tetrahedron and a 4 sites unit cell.

A continuum of states with a non-zero total magnetization partially breaks $O(3)$ ($H_c^S = \mathbb{Z}_2$):

- the V states of Fig. 5(e), which interpolate between the F and AF states.

C. Square lattice

The symmetry group S_L of the square lattice is distinct from that of the triangular lattice (see Fig. 2) and one has to determine its algebraic symmetry groups from a system of equations similar to Eqs. 7. The 168 solutions are listed below:

$$
\begin{aligned}
G_{T_1} = G_{T_2} = \varepsilon_1 I, G_\sigma = \varepsilon_\sigma R_{z\pi}, G_{R_4} = \varepsilon_R R_{x\pi},\\
G_{T_1} = G_{T_2} = \varepsilon_1 R_{\mathbf{z}\pi\delta_1}, G_\sigma = \varepsilon_\sigma R_{\mathbf{x}\pi}, G_{R_4} = \varepsilon_R R_{\mathbf{z}\frac{\pi}{2}},\\
G_{T_1} = G_{T_2} = \varepsilon_1 R_{\mathbf{z}\pi\delta_1}, G_\sigma = \varepsilon_\sigma R_{\mathbf{z}\pi\delta_\sigma}, G_{R_4} = \varepsilon_R R_{\mathbf{z}\pi\delta_R},\\
G_{T_1} = G_{T_2} = \varepsilon_1 R_{\mathbf{z}\pi}, G_\sigma = \varepsilon_\sigma R_{\mathbf{z}\pi\delta_\sigma}, G_{R_4} = \varepsilon_R R_{\mathbf{x}\pi},\\
G_{T_1} = G_{T_2} = \varepsilon_1 R_{\mathbf{z}\pi}, G_\sigma = \varepsilon_\sigma R_{\mathbf{x}\pi}, G_{R_4} = \varepsilon_R R_{\mathbf{z}\pi\delta_R},\\
G_{T_1} = G_{T_2} = \varepsilon_1 R_{\mathbf{z}\pi}, G_\sigma = \varepsilon_\sigma R_{\mathbf{x}\pi}, G_{R_4} = \varepsilon_R R_{\mathbf{x}\pi},\\
G_{T_1} = G_{T_2} = \varepsilon_1 R_{\mathbf{z}\pi}, G_\sigma = \varepsilon_\sigma R_{\mathbf{x}\pi}, G_{R_4} = \varepsilon_R R_{\mathbf{y}\pi},\\
G_{T_1} = \varepsilon_1 R_{\mathbf{x}\pi}, G_{T_2} = \varepsilon_1 R_{\mathbf{y}\pi},\\
G_\sigma = \begin{pmatrix} 0 & 1 & 0 \\ 1 & 0 & 0 \\ 0 & 0 & -\varepsilon_\sigma \end{pmatrix}, G_{R_4} = \begin{pmatrix} 0 & e_1 & 0 \\ e_2 & 0 & 0 \\ 0 & 0 & e_3 \end{pmatrix},
\end{aligned}
$$

where $\mathbf{x}$, $\mathbf{y}$, $\mathbf{z}$ are orthonormal vectors, e_1, e_2, e_3, ε_1, ε_σ, $\varepsilon_R = \pm 1$ and δ_R, δ_σ, $\delta_1 = 0$ or 1.

Then, the construction of the compatible states leads to the RMOs depicted in Fig. 6 and listed below.

Two RMOs are colinear ($H_c^S = O(2)$):

- the ferromagnetic state of Fig. 6(a),
- the (π, π) Néel (AF) state of Fig. 6(b) has 2 sublattices of spins oriented in opposite directions and a 2 sites unit cell.

One state with a zero total magnetization is coplanar ($H_c^S = \mathbb{Z}_2$):

- the orthogonal coplanar state of Fig. 6(c) has 4 sublattices of spins with angles of 90° and a 4 sites unit cell.

Then we have three continua of states with different spin symmetry group H_c^S :

- the V states of Fig. 6(d) have a non-zero total magnetization and partially break $O(3)$ ($H_c^S = \mathbb{Z}_2$). They interpolate between the F and the (π, π) Néel states,

- the tetrahedral umbrella states of Fig. 6(e) have a zero total magnetization and completely break $O(3)$ ($H_c^S = \{I\}$). They interpolate between the (π, π) Néel and the orthogonal coplanar state,
- the 4-sublattice umbrella states of Fig. 6(f) have a non-zero total magnetization and completely break $O(3)$ ($H_c^S = \{I\}$). They interpolate between the F and the orthogonal coplanar state.

D. Regular magnetic orders with only translations

When the lattice symmetry group is commutative, the construction of RMOs is particularly simple. This occurs if only translations are considered. In that case, one may chose some arbitrary directions for the spins of the reference unit cell. Then, one has to chose an $O(3)$ element G_{T_i} associated to each unit lattice translation T_i in direction i (with as many generators as space dimensions). Assuming that $H_c^S = I$, and using the fact that the translations commute with each other, we find that the G_{T_i} also commute. A first family of solutions consists in choosing a set of rotations with the same axis $\mathbf{n}$, and unconstrained angles. This gives the conventional spiral states. Thanks to the arbitrary choice of the spin directions in the reference unit cell, such states are not necessarily planar.

All these solutions may be generalized by combining one or more G_{T_i} with a spin inversion $-I$. These generalized spiral states will be noted SSs in the following.

Finally, an other family of solutions can be obtained by choosing the G_{T_i} among the set of π-rotations with respect to some orthogonal spin directions, therefore insuring the commutativity, combined or not with $-I$.

V. GEOMETRICAL REMARKS

In this section, we discuss some geometrical properties of RMOs.

A. Groups and polyhedra

From a RMO c, one can consider the set $\Sigma \subset \mathcal{A}$ of all the different orientations taken by the spins. We assume that c has a finite number of sublattices/spin directions, so that Σ is finite. For a three-component spin system, Σ is just a set of points on the unit sphere $\mathcal{S}_2$, as displayed in central columns of Figs. 3, 4, 5 and 6. Σ may be a single site, the ends of a segment, the corners of a polygon or of a polyhedra.

The four lattices studied here share some special properties: all the sites and all first-neighbors bonds are equivalent (linked by a S_L transformation). Due to this equivalence, Σ also form a segment/polygon/polyhedron with equivalent vertices and bonds.[35] A polyhedron with this property is said to be quasi-regular. If the elementary plaquettes of the lattices are also equivalent (as in the triangular, square and hexagonal lattices, but not in the kagome lattice where both triangular and hexagonal

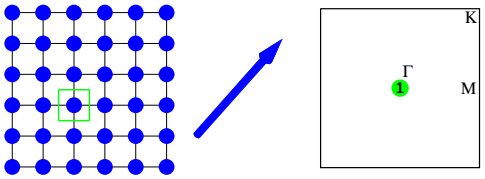

(a) Ferromagnetic (F) state.
$E = 4J_1 + 4J_2 + 4J_3 + 14K$.

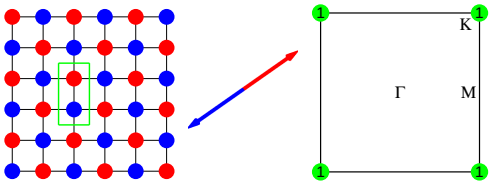

(b) (π, π) Néel (AF) state.
$E = -4J_1 + 4J_2 + 4J_3 - 2K$.

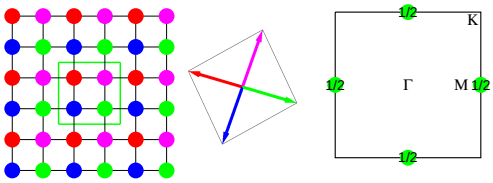

(c) Orthogonal coplanar state.
$E = -4J_2 + 4J_3 - 6K$.

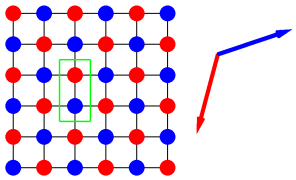

(d) V states.

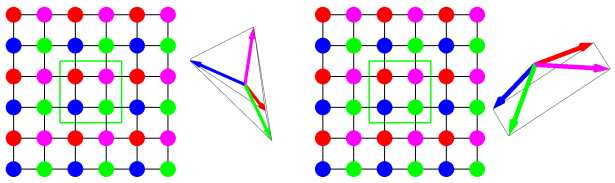

(e) Tetrahedral umbrella states (*AF umbrellas*).

(f) Umbrella states (*F umbrellas*).

FIG. 6: (Color online) Regular magnetic orders on the square lattice and their equal time structure factors in the square BZ. The energy per site of each structure is given as a function of the parameters of the models described in Sec VI.

elementary plaquettes are present) and if Σ is a polyhedron, its faces should also be equivalent. Σ must then be one of the five regular convex polyhedra (Platonic solids):[17] tetrahedron, cube, octahedron, dodecahedron or icosahedron.[36]

We now only consider the case where $H_c^S = \{I\}$ (this condition can always be verified by reducing $\mathcal{A}$ to its elements invariant by H_c^S and by consequently modifying S_S). Clearly, the lattice symmetries constraint the possibilities for the set Σ, since each lattice symmetry X permutes the sites in Σ but leaves it globally unchanged.[37] But since the state c is regular, these permutations can also be achieved by a spin symmetry in S_S, and the symmetry group S_Σ of Σ should be viewed as a finite subgroup of S_S.

For $S_S = O(3)$, the classification of these subgroups – called point groups – is a classical result in geometry,[17] it contains seven groups (related to the three symmetry groups of the five regular polyhedra) and seven infinite series (conventionally noted C_n, C_{nv}, C_{nh}, D_n D_{nh} D_{nd} and S_n with $n \in \mathbb{N}$. They are related to the cyclic and dihedral groups). Of course, the non planar RMOs we have discussed so far (Sec. III C and IV) fall into this classification. For instance, the three- and four- sublattice umbrella states of Fig. 3(d), 6(e) and 6(f) correspond to C_{3v}, D_{2d} and C_{4v} (with respectively 6, 8 and 8 elements). The cubic, octahedral and cuboctahedronl states correspond to the symmetry group of the cube (48 elements), and the tetrahedral state corresponds (of course) to its own symmetry group.

B. Regular magnetic orders and representation of the lattice symmetry group

We again focus on three-component spin systems with a spin symmetry group $S_S = O(3)$. In a RMO c each lattice symmetry X can be associated to a matrix G_X in $O(3)$. Now, as in Sec. III A, we can compare the actions of two lattice symmetries X and Y. $G_X G_Y G_{XY}^{-1}$ belongs to H_c^S. By chosing G_X invariant in all directions perpendicular to all spins, we obtain $G_X G_Y = G_{XY}$, which implies that G is a *representation* of the lattice symmetry group S_L. After removing the trivial representations associated to directions perpendicular to spins, its dimension is 1 for a colinear state, 2 for planar states, and 3 for the others. Is this representation reducible ? If yes, it must contain at least one representation of dimension 1 (because the maximal dimension considered here is 3), thus there exist at least one spin direction which is stable under all the spin symmetry operations spanned by G_X with $X \in S_L$. Except in the trivial colinear case, one can easily check that it is the case only for the states belonging to a continuum. For the V-states, G is the direct sum of a trivial and a non trivial 1d representation of S_L. For the umbrella states, G is the direct sum of a trivial 1d and a 2d irreducible representation (IR). For the tetrahedral state of Fig. 6(e), G is the direct sum of a non-trivial 1d and a 2d IR representation. For the other cases, the associated representation is irreducible.

There is another context where antiferromagnetic Néel states are known to be related to irreducible representations. If a quantum antiferromagnet has a GS with long-range Néel order, its spectrum displays a special structure, called "tower of states".[5,6] It reflects the fact that a symmetry breaking Néel state is a linear combination of specific eigenstates with different quantum numbers describing the spatial symmetry breaking, and with different values of the total spin S, describing the $SU(2)$ symmetry breaking. If such a quantum system has a GS with a regular Néel order, its tower of state should have an $S = 1$ state with the same quantum numbers as those of the irreducible representation $X \mapsto G_X$ discussed above. The reason why this representation shows up in the $S = 1$ sector of the tower of state is because $S = 1$ corresponds to the action of the lattice symmetries onto a three-dimensional vector, as the classical spin directions.

VI. ENERGETICS

As discussed in the introduction, there is no simple way to find the GS of a classical spin model if the lattice is not a Bravais lattice, and/or if spin-spin interactions are not simply quadratic in the spin components. So far, we have discussed RMOs from pure symmetry considerations, but in Sec. VI A we show that, under some rather general conditions, a RMO is a *stationary* point for the energy, whatever the Hamiltonian (provided it commutes with the lattice symmetries).

In addition, we argue that RMOs are good candidates to be *global energy minima*. To justify this, we first discuss a rigorous energy lower bound (Sec. VI B) for Heisenberg like Hamiltonians and investigate in Sec. VI C several Heisenberg models with further neighbor interactions (J_1, J_2, J_3, etc.) on non-Bravais lattices such as the hexagonal and kagome lattices. In large regions of the phase diagrams, one RMO energy reaches the lower bound and is one (may be not unique) exact GS.

A. A condition for a RMO to be "stationary" with respect to small spin deviations

To address the question of energetic stability of RMOs, we give some conditions under which an infinitesimal variation of the spin directions would not change the energy (necessary condition to have a GS). To simplify the notations we consider an Heisenberg model with some competing interactions (such as in Eq.(1)), but the arguments easily generalize to multi-spin interactions of the form $(\mathbf{S}_i \cdot \mathbf{S}_j)(\mathbf{S}_k \cdot \mathbf{S}_l) \dots$ (respecting the lattice symmetries).

We assume that there is a non trivial lattice symmetry X which leaves one site i unchanged: $X(i) = i$ (existence

of a non-trivial point group). In addition, we assume that a spin rotation R_s of axis $\mathbf{n}$ and angle $\theta \neq 0$ can be associated to X in order to have $R_s X c = c$. These conditions insure that the invariant direction of R_s is $\mathbf{n} = \pm\mathbf{S}_i$. Excepted states belonging to a continuum, all RMOs verify these conditions on the lattices we have studied .

With these conditions, the derivatives of the energy with respect to the spin directions vanish. The proof is as follows. One considers the local field $\mathbf{h}_i = \frac{\partial E}{\partial \mathbf{S}_i}$ which is experienced by the spin i. $\mathbf{h}_i$ is a linear combination of the $\mathbf{S}_j$ where j runs over the sites which interact with the site i:

$$\mathbf{h}_i = \sum_d J_d \sum_{j \in N_d(i)} \mathbf{S}_j, \tag{12}$$

where $N_d(i)$ is the set of the neighbors of i at distance d on the lattice. Since the configuration c is invariant under $R_s X$, one may also compute $\mathbf{h}_i$ as

$$\mathbf{h}_i = \sum_d J_d \sum_{j \in X(N_d(i))} R_s(\mathbf{S}_j). \tag{13}$$

X reshuffles the neighbors of i (at any fixed distance) but since $X(i) = i$, $N_d(i)$ is globally stable: $N_d(i) = X(N_d(i))$. So, from Eq. (13), we have

$$\mathbf{h}_i = R_s(\mathbf{h}_i). \tag{14}$$

We therefore conclude that $\mathbf{h}_i$ is colinear with $\mathbf{n}$ and thus colinear with $\mathbf{S}_i$. This shows that the energy derivative $\frac{\partial E}{\partial \mathbf{S}_i}$ vanishes for spin variations orthogonal to $\mathbf{S}_i$ (longitudinal spin variations are not allowed as $(\mathbf{S}_i)^2$ must be kept fixed).

All RMOs studied in the previous examples that do not belong to a continuum are thus energetically stationnary with respect to small spin deviations. They are thus interesting candidates for global energy minima.

B. Lower bound on the energy of Heisenberg models

The Fourier transform $\mathbf{S}_{\mathbf{q}i}$ of the local spin on a periodic lattice of N unit cells is defined by

$$\mathbf{S}_{\mathbf{q}i} = \frac{1}{\sqrt{N}} \sum_{\mathbf{x}} \mathbf{S}_{\mathbf{x}i} e^{-i\mathbf{q}\mathbf{x}}.$$

where each site is labeled by an index $i = 1 \dots m$ (m is the number of sites per unit cell), $\mathbf{x}$ is the position of its unit cell, and $\mathbf{q}$ is a wave vector in the first Brillouin zone. For an Hamiltonian in the form of Eq. (1), the energy can be written as:

$$E = \sum_{\substack{\mathbf{v},\mathbf{x} \\ i,j=1,\dots,m}} J_{ij}(\mathbf{v})\, \mathbf{S}_{\mathbf{x}i} \cdot \mathbf{S}_{\mathbf{x}+\mathbf{v}j} \tag{15}$$

$$= \sum_{\substack{\mathbf{q} \in \mathrm{BZ} \\ i,j=1,\dots,m}} J_{ij}(\mathbf{q})\, \mathbf{S}_{-\mathbf{q}i} \cdot \mathbf{S}_{\mathbf{q}j} \ , \tag{16}$$

with

$$J_{ij}(\mathbf{q}) = \sum_{\mathbf{v}} J_{ij}(\mathbf{v}) e^{i\mathbf{q}\mathbf{v}}. \tag{17}$$

Since $(\mathbf{S}_{i\mathbf{x}})^2 = 1$ for all i and $\mathbf{x}$, $\sum_{i\mathbf{x}} \mathbf{S}_{i\mathbf{x}}^2 = \sum_{i\mathbf{q}} \mathbf{S}_{q\mathbf{x}}^2 = mN$, we see that a lower bound on the energy (per site) is obtained from the lowest eigenvalue of the matrices $J(\mathbf{q})$:[7]

$$\frac{E}{mN} \geq \min_{\{\mathbf{q}\}} \left(J_{\mathbf{q}}^{\min}\right) \tag{18}$$

where $J_{\mathbf{q}}^{\min}$ is the lowest eigenvalue of the matrix $J(\mathbf{q})$.

If the lattice has a single site per unit cell ($m = 1$) this lower bound is reached by a planar spiral of the form:[1]

$$\mathbf{S}_{\mathbf{x}1} = \mathbf{u}\cos(\mathbf{Q}\cdot\mathbf{x}) + \mathbf{v}\cos(\mathbf{Q}\cdot\mathbf{x}) \tag{19}$$

where $\mathbf{Q}$ is the propagation vector (pitch) of the spiral, and corresponds to a minimum of $J_{\mathbf{q}}^{\min}$. In spin space, the plane of the spiral is fixed by two orthonormal vectors $\mathbf{u}$ and $\mathbf{v}$. When $m = 1$, it is only when $J_{\mathbf{q}}^{\min}$ admits several degenerate minima in the Brillouin zone that additional non-spiral (and possibly non-planar) GS may be constructed. If the lattice has more than one site per unit cell, an attempt to construct a spiral with a pitch corresponding to the smallest eigenvalue $J(\mathbf{Q})^{\min}$ will generally *not* lead to a physical spin configuration with fixed spin length $\mathbf{S}_{i\mathbf{x}}^2 = 1$ at every site. We will however see in the next section that for some models, a non-planar RMO may reach the lower bound, whereas all the spiral states are energetically higher.

C. Variational phase diagrams of Heisenberg models on the kagome and hexagonal lattices

In this section we comment the phase diagrams of J_1-J_2-J_3(-J_3') Heisenberg models on the kagome and hexagonal lattices. J_n is the interaction between n^{th} neighbors. On the kagome lattice, there are two types of third neighbors depicted in Fig. 8(a), and thus two coupling constants J_3 and J_3'.

For each set of parameters, we determined the lowest energy RMO (the energies of RMOs are given in Figs. 4 and 5), the lowest energy SS of Sec. IV D and the lower bound on the energy. The results on these two lattices are described in Figs. 7 and 8. Such phase diagrams are *a priori* variational. However, it turns out than in all the colored (white included, grey and black excluded) regions of Figs. 7 and 8, the RMO with the lowest energy reaches the rigorous lower energy bound of Eq. (18). *This demonstrates that (at least) one GS is regular in these regions of the parameter space.* In the grey areas, the energy lower bound is not reached, but the regular near-by state could be a GS as no SS has a lower energy. In the black areas, the GS is not regular: some SS is energetically lower (but sometimes still higher than the lower bound). All

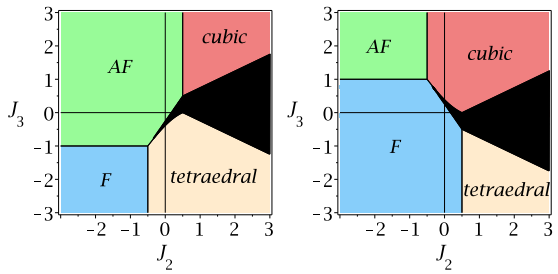

(a) $J_1 = 1$ (AF) (b) $J_1 = -1$ (F)

FIG. 7: (Color online) Phase diagram of the J_1-J_2-J_3 Heisenberg model on the honeycomb lattice. Labels refer to the RMOs described in Fig.5. In each colored region (black excluded), the RMO is an exact GS. In the black region a generalized spiral state (SS) has an energy stricly lower than the RMOs, but the actual GS energy might still be lower.

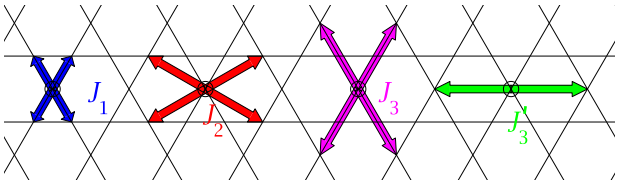

(a) Definition of the coupling constants of the model.

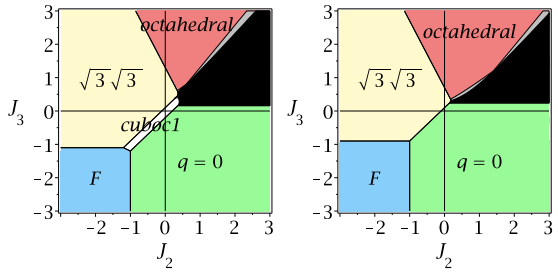

(b) $J_1 = 1$, $J'_3 = 0.2$ (c) $J_1 = 1$, $J'_3 = -0.2$

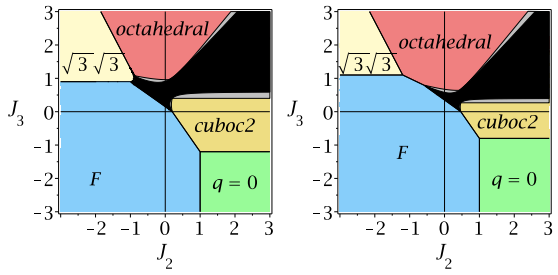

(d) $J_1 = -1$, $J'_3 = 0.2$ (e) $J_1 = -1$, $J'_3 = -0.2$

FIG. 8: (Color online) Phase diagram of the J_1-J_2-J_3-J'_3 model on the kagome lattice. In each colored region (white included, grey and black excluded), the RMO is an exact GS. Labels refer to the RMOs described in Fig.4. In the grey regions, the near-by RMO does not reach the lower bound of Sec. VI B but no SS is energetically lower. In the black regions, a SS has a lower energy than the RMOs, but the actual GS might yet be lower.

RMOs (excepted those from continua) appear in some area of the presented phase diagrams. This shows that these states are good candidates as variational GSs. The absence of RMOs of a continuum in an Heisenberg model is easily understood. The energy E of any RMO c belonging to a continuum cannot be lower than the energies E_1 and E_2 of the two states c_1 and c_2 between which it interpolates. One (at least) of the two states, say c_1, is colinear along a direction $\mathbf{n}$. The c_2 spins are then perpendicular to $\mathbf{n}$. Let θ be the angle between the spins of the continuum state and $\mathbf{n}$. Then $\mathbf{S}_i = \mathbf{S}_i^{c_1}\cos\theta + \mathbf{S}_i^{c_2}\sin\theta$ and the energy reads $E = E_2 + (E_1 - E_2)\cos^2\theta$. Thus, E is in between E_1 and E_2 and is never strictly the lowest energy.[38]

We will now address the possible degeneracies of regular tridimensionnal spin states in these models. On the hexagonal lattice, our phase diagram is in agreement with Ref. 10. One should nevertheless notice that the regular tridimensionnal orders (tetrahedral and cubic states) are degenerate with colinear non RMOs. These last states have a higher density of soft excitations (larger energy wells in the phase space landscape) and will always win as soon as (thermal or quantum) fluctuations are introduced (order by disorder mechanism[11–15]). However the non planar configurations could be stabilized by quartic or ring-exchange interactions.

On the kagome lattice (Fig. 8) the occurrence of the cuboc2 (Fig. 4(f)) for J_1-J_2 interactions[16] and of the cuboc1 (Fig. 4(e)) for J_1-J'_3 interactions[19] has already been reported. These two states are not degenerated with SSs and are to our knowledge unique and stable GSs of the model. To our knowledge, the octahedral state has not been found before, but this state has the same energy as a continuum of non SSs including colinear states, and it will be destabilized by any fluctuation.

D. Square and triangular lattices: Phase diagrams of Heisenberg versus ring-exchange models

In this section we will comment the phase diagram of the Heisenberg models (Eq. (1)) on the square and triangular lattices and display the effect of 4-spin ring-exchange (J_1-J_2-K) on these two lattices. The J_1-J_2-K model is defined as:

$$E = \sum_{i,j} J(|\mathbf{x}_i - \mathbf{x}_j|)\mathbf{S}_i\cdot\mathbf{S}_j + K\sum_{i,j,k,l}((\mathbf{S}_i\cdot\mathbf{S}_j)(\mathbf{S}_k\cdot\mathbf{S}_l) + (\mathbf{S}_i\cdot\mathbf{S}_l)(\mathbf{S}_j\cdot\mathbf{S}_k) - (\mathbf{S}_i\cdot\mathbf{S}_k)(\mathbf{S}_j\cdot\mathbf{S}_l) + \mathbf{S}_i\cdot\mathbf{S}_j + \mathbf{S}_j\cdot\mathbf{S}_k + \mathbf{S}_k\cdot\mathbf{S}_l + \mathbf{S}_l\cdot\mathbf{S}_i + \mathbf{S}_i\cdot\mathbf{S}_k + \mathbf{S}_j\cdot\mathbf{S}_l) \quad (20)$$

where the sum in the K term runs on rhombi i,j,k,l.[2] This model encompasses first and second neighbor J_1 and J_2 couplings and a K ring-exchange term which introduces quartic interactions as well as modifications of first and second neighbor Heisenberg interactions.[2] The phase diagramms are displayed in Figs: 9 and 10.

In the J_1-J_2-J_3 Heisenberg phase diagrams on the square and triangular lattice, all RMOs that do not be-

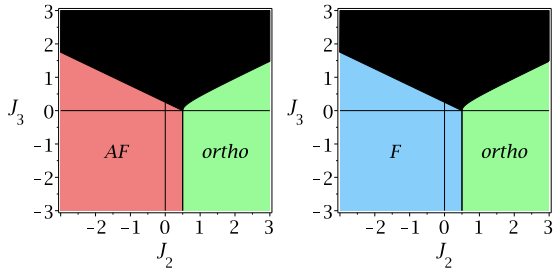

(a) $J_1 = 1$ (AF) (b) $J_1 = -1$ (F)

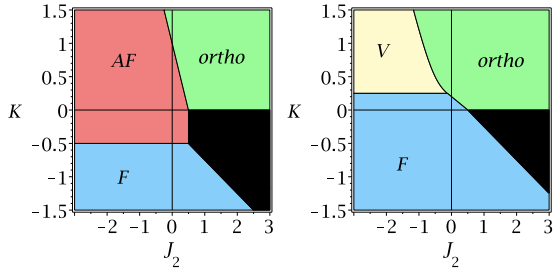

(c) $J_1 = 1$ (AF) (d) $J_1 = -1$ (F)

FIG. 9: (Color online) Phase diagrams on the square lattice with J_1-J_2-J_3 Heisenberg interactions (top line) and J_1-J_2-K model (bottom line). Labels refer to RMOs defined in Fig. 6. In each colored region (black excepted), the RMO has the lowest energy of the set of all regular and generalized spiral states. In the black regions, a SS has a lower energy than the RMOs. For pure Heisenberg interactions, we know that we obtain the GS energy, but for non Heisenberg interactions the actual GS might be lower. In the J_1-J_2-J_3 model the coplanar (orthogonal 4-sublattice) phase is degenerate with non regular colinear states, which will win upon introductions of fluctuations. A contrario the coplanar (orthogonal 4-sublattice) phase is stable in a large range of parameters in the J_1-J_2-K model.

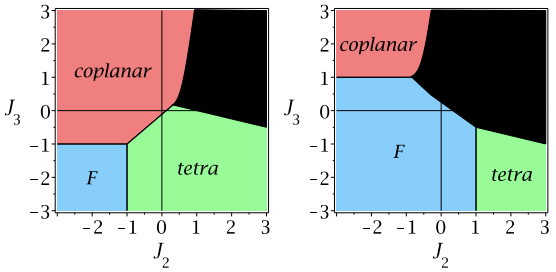

(a) $J_1 = 1$ (AF) (b) $J_1 = -1$ (F)

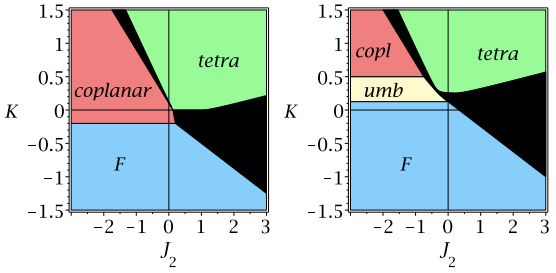

(c) $J_1 = 1$ (AF) (d) $J_1 = -1$ (F)

FIG. 10: (Color online) Phase diagrams on the triangular lattice with J_1-J_2-J_3 Heisenberg interactions (top line) and J_1-J_2-K model (bottom line). Labels refer to RMOs defined in Fig. 3. In each colored region (black excepted), the RMO has the lowest energy of the set of all regular and generalized spiral states. In the black regions, a SS has a lower energy than the RMOs. For pure Heisenberg interactions, we know that we obtain the GS energy, but for non Heisenberg interactions the actual GS might be lower.

long to continua do appear as an exact GS in some parts of the phase diagrams (colored regions - black excepted of Figs. 9(a), 9(b), 10(a) and 10(b)). In black regions, SSs are more stable than RMOs. As these lattices are Bravais lattices, we know how to reach the lower bond of Sec. VI B thanks to a spiral state. The orthogonal state on the square lattice and the tetrahedral state on the triangular lattice (Fig. 3(b) and 6(c)) are degenerate with SSs including colinear states with 2 spins (up, down) in the magnetic unit cell, which will win upon introduction of fluctuations. On a large part of the phase diagram on the square lattice (spirals excepted) the spins are thus colinear.

The presence of a 4-spin ring exchange on the square lattice gives richer phase diagramms (Figs. 9(c) and 9(d)) with the appearance of states from continua. We recall that these phase diagrams are variational and give the minimal energy state among the regular and the generalized spiral states. A dominant 4-spin ring exchange stabilizes the orthogonal 4-sublattice coplanar antiferromagnet, which is known to be robust to large quantum fluctuations.[20] One of these phases belongs to a continuum: the V states (Fig: 6(d)). Part of this phase diagram on the square lattice has been known for a long time for the J_1-K model,[21] but the effect of a second neighbor interaction leads to new phases that might be interesting in various respects.

The J_1-J_2-K phase diagramm on the triangular lattice (Figs. 10(c) and 10(d)) exhibits all the regular phases that can be constructed on this lattice. In that model, large ring-exchange stabilizes the tetrahedral chiral phase studied by Momoi and co-workers.[2,22] The presence of large parts of the phase diagramms with planar or 3-dimensional order parameter at $T = 0$, and of points where a large number of classical phases are in competition, could give interesting hints in the quest of exotic quantum phases.[23–25]

E. Finite temperature phase transitions in two-dimensions

In two-dimensions, the Mermin-Wagner[26] theorem insures that continuous symmetries cannot be spontaneously broken at finite temperature. It does however

not prevent discrete symmetries to be broken. Indeed, some finite temperature phase transitions associated to discrete symmetries have been found in classical $O(3)$ models: lattice symmetry breaking in the J_1-J_2 and J_1-J_3 models on the square lattice,[27–29] chiral symmetry breaking in a ring-exchange model on the triangular lattice[15,22] and in a J_1-J_2 model on the kagome lattice.[16,30]

What should be expected in a system where the GS is a RMO c ? Let us first consider the case where c is not chiral, that is when the spin inversion $\mathbf{S} \to -\mathbf{S}$ gives a state c' which can also be obtained from c by a rotation in $SO(3)$. At an infinitesimal temperature, the rotational symmetry is restored and the statistical ensemble is that of all the (regular) states obtained from c by $SO(3)$ rotations. The thermal average of an observable is therefore also an average over $SO(3)$ rotations. Now, if we compare an observable O and the same observable after a lattice symmetry X, we will get the same average (for RMOs, the effect of X can be absorbed by a rotation). So not only the rotational symmetries, but all the lattice symmetries are restored at $T = 0^+$. The simplest scenario is therefore a complete absence of symmetry-breaking phase transition from $T = 0^+$ up to $T = \infty$. Now, for a chiral state, the thermal fluctuations will only partially restore the $O(3)$ symmetry of the model, and a chiral phase transition should be expected. From this point of view, a classical system in two-dimensions with no finite-temperature phase transition is likely to have a regular and non-chiral GS.

When some magnetic long-range order develops, the magneto-elastic couplings often drive the system to a small but detectable (through X-ray diffraction for instance) lattice distortion. This generically happens if the magnetic order induces some inequivalent bonds, since the magnetic energy gain is then expected to be linear in the displacements, whereas the elastic energy cost is quadratic. However, such inequivalent bonds do not occur in the case of RMOs (the energy is rotationally invariant, hence uniform) and we expect the crystal to keep its full symmetry in such a magnetically ordered phase. Likewise, the absence of any lattice distortion down to zero temperature can be used as an (experimental) indication that the magnetic phase is regular.

VII. CONCLUSION

Based on symmetry considerations (and on an analogy with Wen's[3] classification of quantum spin liquids using the concept of PSG), we introduced a family of classical magnetic structures, dubbed "regular" magnetic orders. They can be constructed in a systematic way for any lattice, in any dimension, for any type of spins, using the method explained in Sec. III. We found that these states are often good variational states to study the zero-temperature phase diagram of "complex" problems (non-Bravais lattice and/or multiple spin interactions for instance). In many cases, one of the RMOs is found to reach a lower energy bound, allowing to show that it is a GS.

We note that, although one can always find a planar GS in Heisenberg models on a Bravais lattice, non-planar spin structures with many sublattices are rather common in presence of competing interactions, non quadratic spin interactions and non-Bravais lattices. As mentioned in the introduction, we believe this approach may find an application in the study of real magnetic compounds where the (equal time) spin-spin correlations are measured, but the strength and range of the magnetic exchange interactions are not known.

We have studied the case where the spin manifold $\mathcal{A} = \mathcal{S}_2$ is that of a three-component spin (unit vector), but other manifolds could be investigated using the same approach. For instance, *regular nematic orders* would be obtained with $\mathcal{A} = \mathcal{S}_2/\mathbb{Z}_2$ and $S_S = SO(3)$.

This approach was applied here to purely classical models, but can be applied similarly to quantum systems where the spin rotational symmetry is broken (magnetic long range order). App. C describes a similar approach for the case of spin *liquids*, where no symmetry at all is broken. It is interesting to understand the connections between RMOs and (mean-field) spin liquids. In particular, an important question is to identify which spin liquid may give rise to which RMO upon spinon condensation. This issue has been addressed in Ref. 32 and will be the subject of a future publication.

Acknowledgments

We thank L. Pierre for enlightening discussions on spiral states and V. Pasquier for interesting input on geometrical considerations and for mentioning Ref. 17. This research was supported in part by the National Science Foundation under Grant No. PHY05-51164.

Appendix A: Derivation of the algebraic symmetry groups on the triangular lattice

In this section, we look for all the algebraic symmetry groups on the triangular lattice with symmetries of Fig. 2. They are the solutions of the system Eq. 8 recalled here:

$$G_{T_1} G_{T_2} = G_{T_2} G_{T_1} \tag{A1a}$$
$$G_{T_1} G_{R_6} G_{T_2} = G_{R_6} \tag{A1b}$$
$$G_{R_6} G_{T_1} G_{T_2} = G_{T_2} G_{R_6} \tag{A1c}$$
$$G_{T_1} G_{\sigma} = G_{\sigma} G_{T_2} \tag{A1d}$$
$$G_{R_6}^6 = I \tag{A1e}$$
$$G_{\sigma^2} = I \tag{A1f}$$
$$G_{R_6} G_{\sigma} G_{R_6} = G_{\sigma}. \tag{A1g}$$

Each element G_X in $O(3)$ is characterised by its determinant $\varepsilon_X = \pm 1$ and by a rotation $R_{\mathbf{n}_X \theta_X}$ of axis $\mathbf{n}_X$ and of angle $\theta_X \in [0, \pi]$ such that $G_X = \varepsilon_X R_{\mathbf{n}_X \theta_X}$.

We choose an orthonormal right-oriented basis $(\mathbf{x},\mathbf{y},\mathbf{z})$ to express the results (such that $\mathbf{x}\cdot(\mathbf{y}\wedge\mathbf{z})=1$).

Some simple conditions on solutions are easily obtained: from Eq. A1c we deduce that $\varepsilon_{T_1}=1$, from Eq. A1b that $\varepsilon_{T_2}=1$. Eq. A1d is a similarity relation thus $\theta_{T_1}=\theta_{T_2}$. Eqs. A1e and A1f gives $6\theta_{R_6}=2\theta_\sigma=0$ modulo 2π. These first results are summarized below:

$$\varepsilon_{T_1}=\varepsilon_{T_2}=1 \tag{A2a}$$
$$\theta_{T_1}=\theta_{T_2} \tag{A2b}$$
$$\theta_\sigma\in\{0,\pi\} \tag{A2c}$$
$$\theta_R\in\left\{0,\frac{\pi}{3},\frac{2\pi}{3},\pi\right\}. \tag{A2d}$$

The values of ε_σ and ε_{R_6} have no influence on the validity of a solution. Thus we solve Eq. A1 only for $\varepsilon_\sigma=\varepsilon_{R_6}=1$ and then obtain all solutions by extending their values $(\varepsilon_\sigma,\varepsilon_{R_6})$ to $(\pm1,\pm1)$, keeping the other parameters $(\theta_X,\mathbf{n}_X)$ fixed.

We will divide the solutions in families depending on the relations between G_{T_1} and G_{T_2}. We immediatly discern the case $\theta_{T_1}=0$ ($G_{T_1}=G_{T_2}=I$). From now, $\theta_{T_1}>0$ thus the directions $\mathbf{n}_{T_1}$ and $\mathbf{n}_{T_2}$ are uniquely defined (with only a sign ambiguity when $\theta_{T_1}=\pi$). Eq. A2a implies that G_{T_1} anf G_{T_2} are rotations and possess at least one eigenvalue equal to 1 along the directions $\mathbf{n}_{T_1}$ and $\mathbf{n}_{T_2}$. Eq. A1a applied to vectors $\mathbf{n}_{T_1}$ gives that $G_{T_2}\mathbf{n}_{T_1}$ is an eigenvector of G_{T_1} with eigenvalue 1. If this vector is linearly independant of $\mathbf{n}_{T_1}$, then we know two independant invariant vectors of G_{T_1}. As the eigenvalue product ε_{T_1} is 1 with two eigenvalues equal to 1, we obtain that $G_{T_1}=I$, what contradicts the hypothesis $\theta_{T_1}>0$. We are let with two possibilities: $G_{T_2}\mathbf{n}_{T_1}=\pm\mathbf{n}_{T_1}$.

If $G_{T_2}\mathbf{n}_{T_1}=-\mathbf{n}_{T_1}$, then $\mathbf{n}_{T_1}$ and $\mathbf{n}_{T_2}$ are two perpendicular eigenvectors of G_{T_2} with eigenvalues -1 and 1. The third direction must correspond to the eigenvalue -1. We obtain that $\theta_1=\pi$.

If $G_{T_2}\mathbf{n}_{T_1}=\mathbf{n}_{T_1}$, then $\mathbf{n}_{T_1}=\pm\mathbf{n}_{T_2}$. Combined with Eq. A2b, it means that $G_{T_1}=G_{T_2}$ with $\theta_{T_1}\in]0,\pi[$ or $G_{T_1}=G_{T_2}^{-1}$ with $\theta_{T_1}\in]0,\pi]$. The second subcase is incompatible with Eq. A1c.

We obtain three families of solutions that will now be explored successively:

$$G_{T_1}=G_{T_2}=I \tag{A3a}$$
$$\theta_{T_1}=\theta_{T_2}=\pi \text{ and } \mathbf{n}_{T_1}\perp\mathbf{n}_{T_2} \tag{A3b}$$
$$G_{T_1}=G_{T_2}\neq I. \tag{A3c}$$

- In the case of Eq. A3a, the remaining constraints are Eqs. A1g, A2c and A2d. We treat separately the two cases of Eq. A2c.

  If $G_\sigma=I$, then the possibilities for θ_R restrict to $\{0,\pi\}$. We set $\mathbf{n}_{R_6}=\mathbf{z}$ and obtain the two solutions:

  $$G_{T_1}=G_{T_2}=I, G_\sigma=I, G_{R_6}=I,$$
  $$G_{T_1}=G_{T_2}=I, G_\sigma=I, G_{R_6}=R_{\mathbf{z}\pi}.$$

  If $G_\sigma=R_{\mathbf{z}\pi}$, we have the easily found solution:

  $$G_{T_1}=G_{T_2}=I, G_\sigma=R_{\mathbf{z}\pi}, G_{R_6}=I,$$

  and solutions with $\theta_{R_6}\neq0$. Then from Eq. A1g we have $G_{R_6}G_\sigma\mathbf{n}_{R_6}=G_\sigma\mathbf{n}_{R_6}$, which implies $R_{\mathbf{z}\pi}\mathbf{n}_{R_6}=\pm\mathbf{n}_{R_6}$. In the "+" case, $\mathbf{n}_{R_6}=\mathbf{z}$ and Eqs. A1g and A2d imply that $\theta_R\in\{0,\pi\}$. In the "−" case, $\mathbf{n}_{R_6}\perp\mathbf{z}$. We choose $\mathbf{n}_{R_6}=\mathbf{x}$. Eq. A1g is verified for each θ_{R_6} of Eq. A2d. Solutions are

  $$G_{T_1}=G_{T_2}=I, G_\sigma=R_{\mathbf{z}\pi}, G_{R_6}=R_{\mathbf{z}\pi},$$
  $$G_{T_1}=G_{T_2}=I, G_\sigma=R_{\mathbf{z}\pi}, G_{R_6}=R_{\mathbf{x}\pi/3},$$
  $$G_{T_1}=G_{T_2}=I, G_\sigma=R_{\mathbf{z}\pi}, G_{R_6}=R_{\mathbf{x}\,2\pi/3},$$
  $$G_{T_1}=G_{T_2}=I, G_\sigma=R_{\mathbf{z}\pi}, G_{R_6}=R_{\mathbf{x}\pi}.$$

- In the case of Eq. A3b, we choose $\mathbf{n}_{T_1}=\mathbf{x}$ and $\mathbf{n}_{T_2}=\mathbf{y}$. Eq. A1b applied to $\mathbf{y}$, A1c applied to $\mathbf{z}$, A1d applied to $\mathbf{y}$ and A1e applied to $\mathbf{y}$ give the following forms for the G_{R_6} and G_σ matrices:

  $$G_{R_6}=\begin{pmatrix}0&e_1&0\\0&0&e_2\\e_1e_2&0&0\end{pmatrix},\quad G_\sigma=\begin{pmatrix}0&e_3&0\\e_3&0&0\\0&0&-1\end{pmatrix}, \tag{A6}$$

  whith e_1, e_2 and e_3 are ±1. From Eq. A1g we find that $e_1=-e_3$. It remains 4 possibilities. But we can take $e_1=e_2=1$ up to a basis change: $(\mathbf{x},\mathbf{y},\mathbf{z})\to(e_2\mathbf{x},e_1e_2\mathbf{y},e_1\mathbf{z})$. Thus:

  $$G_{T_1}=R_{\mathbf{x}\pi}, G_{T_2}=R_{\mathbf{y}\pi},$$
  $$G_\sigma=-\begin{pmatrix}0&1&0\\1&0&0\\0&0&1\end{pmatrix}, G_{R_6}=\begin{pmatrix}0&1&0\\0&0&1\\1&0&0\end{pmatrix}.$$

- In the last case of Eq. A3c, we choose $\mathbf{n}_1=\mathbf{z}$. Combining Eqs. A1b and A1c, we obtain that $G_{T_1}^3=I$, Thus, $G_{T_1}=G_{T_2}=R_{\mathbf{z}\frac{2\pi}{3}}$ We treat separately the two cases of Eq. A2c.

  If $G_\sigma=I$, then Eqs. A1b and A1g imply $\theta_{R_6}=\pi$. Eq. A1b applied to $\mathbf{z}$ gives $G_{R_6}\mathbf{z}=\pm\mathbf{z}$ The "+" case ($\mathbf{n}_{R_6}=\pm\mathbf{z}$) contradicts Eq. A1b, so it remains the "−" case: we choose $\mathbf{n}_{R_6}=\mathbf{x}$, which is a solution:

  $$G_{T_1}=G_{T_2}=R_{\mathbf{z}\frac{2\pi}{3}}, G_\sigma=I, G_{R_6}=R_{\mathbf{x}\pi}.$$

  If $\theta_\sigma=\pi$, Eq. A1d implies that $G_\sigma\mathbf{z}=\pm\mathbf{z}$. G_σ is either $R_{\mathbf{z}\pi}$ or a rotation of π around an axe perpendicular to $\mathbf{z}$, say $\mathbf{x}$. This last case contradicts Eq. A1d. The only possibility is thus $G_\sigma=R_{\mathbf{z}\pi}$. From Eq. A1b we know that $G_{R_6}\mathbf{z}=\pm\mathbf{z}$. In the "+" case ($\mathbf{n}_{R_6}=\pm\mathbf{z}$), G_{R_6}, G_{T1} and G_{T2} commute and Eq. A1b is not verified. We set $\mathbf{n}_{R_6}=\mathbf{x}$. From Eq. A2d, only $\theta_{R_6}=\pi$ verify all the equations, giving the unique solution:

  $$G_{T_1}=G_{T_2}=R_{\mathbf{z}\frac{2\pi}{3}}, G_\sigma=R_{\mathbf{z}\pi}, G_{R_6}=R_{\mathbf{x}\pi}.$$

By taking into account the 4 solutions deriving of each of the previous one by multipling G_σ and G_{R_6} by ±1, we finally obtained the list of solutions of Eq. 10.

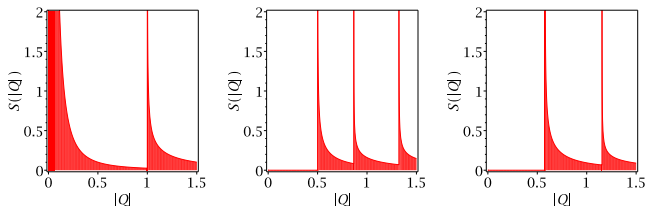

(a) F state (b) Tetrahedral state (c) Coplanar state

FIG. 11: Powder-averaged equal time structure factors $S(|\mathbf{Q}|)$ of the RMOs on the triangular lattice ($|\mathbf{Q}|$ is in units of 2π, $S(|\mathbf{Q}|)$ in arbitrary units).

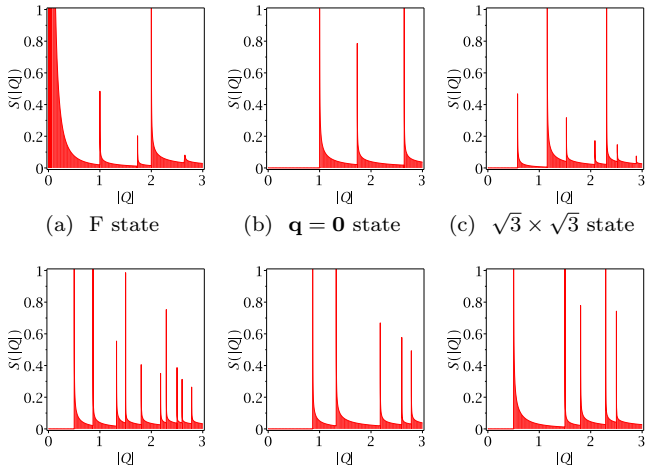

(a) F state (b) $\mathbf{q}=\mathbf{0}$ state (c) $\sqrt{3}\times\sqrt{3}$ state

(d) Octahedral state (e) Cuboc1 state (f) Cuboc2 state

FIG. 12: Powder-averaged equal time structure factors $S(|\mathbf{Q}|)$ of the RMOs on the kagome lattice ($|\mathbf{Q}|$ is in units of 2π, $S(|\mathbf{Q}|)$ in arbitrary units).

Appendix B: Powder-averaged structure factors of regular magnetic orders

Equal time spin-spin correlations partially characterize a spin state and are independent of the energetic properties of the system. Equal time structure factors can thus be analytically calculated on RMOs to form a set of reference neutron scattering results. They can be used to analyze measurements done on compounds with unknown GS. We define the equal time structure factor $S(\mathbf{Q})$ of a state as

$$S(\mathbf{Q}) \propto \sum_{i,j} e^{-i\mathbf{Q}(\mathbf{x}_i-\mathbf{x}_j)}\mathbf{S}_i\cdot\mathbf{S}_j, \tag{B1}$$

where $\mathbf{x}_i$ is the position vector of the site i. The proportionality factor is adjusted to verify the sum rule $\sum_{\mathbf{Q}} S(\mathbf{Q}) = 1$. For perfect long-range orders, $S(\mathbf{Q})$ is zero everywhere except for a finite number of $\mathbf{Q}$ where Bragg peaks are present. They are broadened when chemical defects, non zero temperature or quantum fluctuations are taken into account.

When only powders are realisable, one can measure the powder equal time structure factor $S(|\mathbf{Q}|)$. It is the average of $S(|\mathbf{Q}|\sin\theta(\mathbf{u}\cos\psi+\mathbf{v}\sin\psi))$ over all the possible 3d orientations of $\mathbf{Q}$, where θ, ψ are the spherical coordinates angles of $\mathbf{Q}$ in the orthonormal basis $(\mathbf{u},\mathbf{v},\mathbf{u}\wedge\mathbf{v})$ with $\mathbf{u}$, $\mathbf{v}$ in the sample plane. Thus

$$S(|\mathbf{Q}|) \propto \int d^2\mathbf{q}\frac{\Theta(|\mathbf{Q}|-|\mathbf{q}|)}{|\mathbf{Q}|\sqrt{|\mathbf{Q}|^2-|\mathbf{q}|^2}}S(\mathbf{q}), \tag{B2}$$

where Θ is the Heaviside step function and $\mathbf{q}$ browses the reciprocal 2d space.

The equal time structure factors $S(\mathbf{Q})$ were given in Fig. 3, 4, 5 and 6 for the RMOs on the triangular, kagome, honeycomb and square lattices. The powder-averaged equal time structure factors $S(|\mathbf{Q}|)$ on the triangular and kagome lattices are shown in Fig. 11 and 12.

	Classical spin models	Quantum Mean-field
State	Regular magnetic order	Physically symmetric Ansatz
Internal symmetry group	S_S (global spin rotation, etc.)	Φ (local gauge transformations)
Symmetry group of a state	H_c	PSG
Unbroken internal symmetries	H_c^S	IGG

TABLE I: Analogy between the construction of RMOs and that of symmetric Ansätze in 3.

Appendix C: Analogy with Wen's Projective symmetry groups (quantum spin models)

For quantum spin-$\frac{1}{2}$ Heisenberg models, a standard mean-field approximation consists in expressing the spin operators in term of fermionic operators $f_{i\alpha}$, where i is a lattice site and $\alpha=\uparrow,\downarrow$ is the spin $\pm1/2$. A mean-field decoupling based on some bond parameters η_{ij} and ξ_{ij} (notations and details to be found in in Ref. 3) can then be performed to make the Hamiltonian quadratic in the fermionic operators.

This theory has a local $SU(2)$ gauge invariance. The set of gauge transformations is denoted by Φ. Physical quantities, which can be expressed using spin operators, are unaffected by a gauge transformation, although η_{ij} and ξ_{ij} are generally modified. A mean-field state is characterized by a set of η_{ij} and ξ_{ij} values, called Ansatz. Two mean-field states do have the same physical observables if they are related by a gauge transformation. The group of transformations (lattice, gauge and combined transformations) that do not modify an Ansatz is called the projective symmetry group (PSG). Its subgroup of

pure gauge transformations is called the invariance gauge group (IGG).[3]

One may be interested in states for which all the physical quantities are invariant under the lattice symmetries. To classify these "uniform" states, one can first fix the IGG and then look for the "algebraic" PSG which obey the constraints derived from the algebraic structure of lattice symmetry group S_L.[3] The actual Ansätze can then be constructed.

Clearly, there is a close correspondence between the construction of RMOs discussed in this paper, and that of symmetric Ansätze. This correspondence is summarized in Tab. I.

[1] J. Villain, J. Phys. Fr. **38**, 385 (1977).
[2] K. Kubo and T. Momoi, Z. Phys. B. Condensed Matter **103**, 485 (1997).
[3] X.-G. Wen, Phys. Rev. B **65**, 165113 (2002).
[4] F. Wang and A. Vishwanath, **74**, 174423 (2006).
[5] B. Bernu, P. Lecheminant, C. Lhuillier, and L. Pierre, Phys. Rev. B **50**, 10048 (1994).
[6] P. Lecheminant, B. Bernu, C. Lhuillier, and L. Pierre, Phys. Rev. B **52**, 6647 (1995).
[7] J. M. Luttinger and L. Tisza, Phys. Rev. **70**, 954 (1946).
[8] M. Roger, Phys. Rev. Lett. **64**, 297 (1990).
[9] A. V. Chubukov and D. I. Golosov, J. Phys. Cond. Matt. **3**, 69 (1991).
[10] J.-B. Fouet, P. Sindzingre, and C. Lhuillier, Eur. Phys. J. B **20**, 241 (2001).
[11] J. Villain, R. Bidaux, J. Carton, and R. Conte, J. Phys. Fr. **41**, 1263 (1980).
[12] E. Shender, Sov. Phys. J.E.T.P. **56**, 178 (1982).
[13] C. L. Henley, Phys. Rev. Lett. **62**, 2056 (1989).
[14] A. Chubukov and T. Jolicoeur, Phys. Rev. B **46**, 11137 (1992).
[15] S. E. Korshunov, Phys. Rev. B **47**, 6165 (1993).
[16] J.-C. Domenge, P. Sindzingre, C. Lhuillier, and L. Pierre, Phys. Rev. B **72**, 024433 (2005).
[17] H. S. M. Coxeter, *Regular Polytopes* (Dover, 1973).
[18] D. B. Litvin, Acta Cryst. **A57**, 729 (2001).
[19] O. Janson, J. Richter, and H. Rosner, Phys. Rev. Lett. **101**, 106403 (2008), and J. Phys.: Conf. Ser. **145**, 012008, 2009.
[20] A. Lauchli, J. C. Domenge, C. Lhuillier, P. Sindzingre, and M. Troyer, Phys. Rev. Lett. **95**, 137206 (2005).
[21] A. Chubukov, E. Gagliano, and C. Balseiro, Phys. Rev. B **45**, 7889 (1992).
[22] T. Momoi, K. Kubo, and K. Niki, Phys. Rev.Lett. **79**, 2081 (1997).
[23] W. LiMing, G. Misguich, P. Sindzingre, and C. Lhuillier, Phys. Rev. B, **62**, 6372 (2000).
[24] O. I. Motrunich, Phys. Rev. B **72**, 045105 (2005).
[25] T. Grover, N. Trivedi, T. Senthil, and P. A. Lee, Phys. Rev. B **81**, 245121 (2010).
[26] N. Mermin and H. Wagner, Phys. Rev. Lett. **17**, 1133 (1966).
[27] P. Chandra, P. Coleman, and A. Larkin, J. Phys. Cond. Matt. **2**, 7933 (1990).
[28] C. Weber, L. Capriotti, G. Misguich, F. Becca, M. Elhajal, and F. Mila, Phys. Rev. Lett. **91**, 177202 (2003).
[29] L. Capriotti and S. Sachdev, Phys. Rev. Lett. **93**, 257206 (2004).
[30] J.-C. Domenge, C. Lhuillier, L. Messio, L. Pierre, and P. Viot, Phys. Rev. B **77**, 172413 (2008).
[31] N. Read and S. Sachdev, Phys. Rev. Lett. **66**, 1773 (1991).
[32] L. Messio, Ph.D. thesis, Université Pierre et Marie Curie, Paris (2010).
[33] Once all the RMOs have been constructed for given lattice and spin symmetries (using a simple group theoretic construction, as explained in Sec. III), one can directly compare their energies for a given microscopic Hamiltonian.
[34] A case where $S_H \neq S_S \times S_L$ is the antiferromagnetic square lattice with a site-dependent magnetic field taking two opposite values on each sublattice. The spin inversion $\mathbf{S}_i \to -\mathbf{S}_i$ is not in S_S, the translation by one lattice spacing is not in S_L, but the composition of both is in S_H. The theory developed in this paper can however be used in this case by replacing S_L by S_H/S_S.
[35] Notice that nearest neighbors on the lattice do not necessarly correspond to nearest neighbor spin directions in spin space.
[36] Again, the plaquettes of the lattice need not to map to the faces of the polyhedron.
[37] This relation is particularly easy to visualize in the case of the tetrahedral state on the triangular lattice, since both the lattice and the polydedron Σ have triangular plaquettes/faces: one can put a tetrahedron with a face posed onto a lattice face. Then, one *roll* the tetrahedron over the lattice to obtain a spin direction at each lattice site. Notice that such a construction would *not* work with a cube on the square lattice (and indeed, there is no such eight-sublattice RMO on the square lattice, see Sec. IV C).
[38] In the presence of an external magnetic field $\mathbf{h}$ and if a one-dimensional representation included in G is ferromagnetic (as it is the case for some umbrella's and for the V-states), $\mathbf{n}$ aligns on $\mathbf{h}$. The energy then reads $E = E_2 + (E_1 - E_2)\cos^2\theta - \mathbf{h}\cos\theta$ and an umbrella state becomes stationnary. It is well known that such structure can be the GS in presence of a magnetic field.[8,9]